Modelling of Seismicity in Southern Pakistan using GIS Techniques

Muhammad Khan (jahangir.khan99@gmail.com)

Full paper

Keywords: Fault response, southern Pakistan, Kernel Density, Earthquake

Posted Date: May 18th, 2020

DOI: https://doi.org/10.21203/rs.3.rs-27523/v1

Modelling of Seismicity in Southern Pakistan using GIS Techniques

Muhammad Jahangir Khan

[1]Department of Earth & Environmental Sciences, Bahria University Karachi Campus, Pakistan
[2]International Institute of Earthquake Engineering and Seismology, Iran

Corresponding Author Email: mjahangir.bukc@bahria.edu.pk

Abstract

This study was aimed to expound spatial association between tectonic earthquakes and individual faults in southern Pakistan. A population of fault lines are exposed to the onshore region located to the north of active Makran subduction zone and within Indus Basin where geophysical prospecting reported neotectonic deformation and faulting. A catalog of earthquakes has been compiled considering the seismic events originated from southern Pakistan and neighboring southeastern Iran, southern Afghanistan and frontal offshore areas. Since, the faulty blocks are extending beyond the international borders, a wide region was outlined for cataloging and thorough screening of fault lines. The catalog has been thoroughly processed by standard procedures necessary for magnitude coherency, main shocks decluttering, magnitude completeness and removal of spatially outlier events etc. GIS-based vectors of fault lines were abstracted by the digitization of regional tectonic lineaments and structural maps. A rigorous effort was made to review available literature to gather updated data of plate kinematics, GPS constraints, relative blocks movement across the faults and rate of fault mechanics (slip-sense) during major events. The weights of evidence method was used to judge the spatial associations between seismic events and populations of faults lines to ascribe 'seismicity index' which ranked the potential faults from I (least active level) to V (highly active level). The SI helped to compare each fault response e.g. seismicity yield, released seismic stresses collinear to the fault line, active or aseismic segments and probabilistic estimate for future sizeable earthquake. Kernel density maps were prepared to allure the vulnerable pockets of the elongated faults for specific magnitude windows. The spatial patterns of earthquakes in southern Pakistan were significant to study the seismogenic potential associated with the active tectonic lineaments and faulted blocks. Spatial analysis of data sets for seismic events suggest stronger spatial associations between earthquake epicenters and faults oriented N-S, and weaker spatial associations of epicenters with some -unknown faults in the plains of Indus Basin.

Key words: Fault response; southern Pakistan; Kernel Density; Earthquake.

Introduction

The plate kinematics contribute to the development of elastic stresses/release of elastic strain along seismotectonic margins of drifting lithospheric mosaic and overlying sedimentary cover. In seismically active regions, the accumulating and/or releasing elastic strain energy weaken the rock strength to support the brittle deformation, thus, borne tectonic earthquakes from interplate and intraplate regions. The seismologists are making efforts to study the seismicity patterns in diversified seismotectonic zones of the southern Pakistan (Aslam and Naseer 2020; Ali and Khan, 2015; Ainuddin et al., 2014). The southern Pakistan is a seismic-mélange wherein earthquake engendering mechanisms are closely associated with the active tectonic margins and their faulted cohorts. Fault zones provide anisotropic medium of geological layers across the fault planes which enable the phenomenon to trap elastic energy in creeping blocks over drifting plates in the region (Mokhtari et al., 2019).

The instrumental data of earthquakes post-1970 and review of studies (Ainuddin et al., 2014; Ul-Hadi et al., 2013; Bilham et al., 2007; Ambraseys and Bilham, 2003; Rajendran and Rajendran, 2001) reported that the major tectonic earthquakes (M_w>7.0) were rocked the study area several times such as Mw 7.7 Awaran earthquake of 2013 September 24; M_w 7.2 Dalbandin earthquake of 2011 January19; M_w 7.7 Bhuj earthquake of 2001 January 26; Mw 8.1 Makran earthquake of 1945 November 27; Mw 7.5 Quetta earthquake of 1935 May 30; Mw 7.3 Mach earthquake of 1931 August 27; M_L 8.0 Kutch earthquake of 1844; 7.7<Mw<7.9 Allah bund earthquake of 1819 June 16; 6.5 <Mw<7.0 of Samawani earthquake of 1668; Mw 7.5 Bhaminabad earthquake of 980; Mw 7.5 Makran earthquake of 325 B.C. However, low-to-moderate magnitude seismicity fill the spatial gap between far-offset epicenters of major events. The earthquakes of 1945 and 325 BC along the Makran coast were largest tsunamigenic earthquakes in the offshore Makran region which engendered tsunami waves striking the Pakistan and Iran coast with 8–9 m high tidal waves that damaged the coastal towns of Balochistan coast (Pararas-Carayannis, 2006; Byrne et al., 1992; Quittmeyer and Jacob, 1979). The Awaran earthquake of 2013 was the strongest earthquake which shaken the southern Pakistan and Iran with hefty amplitudes (Ul-Hadi et al., 2013; Ali and Khan, 2015). The epicenters of these seismic events were found closely located to the vulnerable parts of known active faults of the Makran and Sindh region. The extension of the fault lines is widely-spread over spatial

coordinates. Thus, it is necessary to study the seismicity patterns in close association with the seismotectonic features i.e. the plate margins and geological faults lines of southern Pakistan.

The southern Pakistan demonstrate the active nuggets of Arabian, Eurasian and Indian plates. These active assemblages are channelizing the elastic stresses through associated network of fault splays, probably, to the offshore and onshore areas of Arabian, Indian and Eurasian plates. The megathrusting Arabian plate underneath Eursian plate at Makran subduction zone (E-W oriented, ~1000 Km long), the Arabian plate grinding it's shoulder with Indian plate at Murray ridge (NE-SW oriented, ~ 1860 Km long), and the colliding Indian- Eurasian plates at Sulaiman- Kirthar ranges (curvilinear NE-SW & E-W oriented, ~ 610 Km long) (Frohling and Szeliga, 2016; Rani et al., 2011; Szeliga et al., 2012; Smith et al., 2013). These seismotectonic features are primitive source of neotectonic deformation and active seismic events (Pararas-Carayannis, 2006; Martin and Kakar, 2012). The dearth of fixed GPS stations, advanced earthquake instrumentation, broad coverage of geophysical imaging, integration of allied datasets, detailed geophysical and rheological findings about brittle lithosphere and beyond it which preclude critical analysis and look-down into dynamic interior (Szeliga et al., 2012; Minshull et al., 2015).

The Geodetic and GPS constraints provide some controls to understand the development of stresses in the faulty blocks of the southern Pakistan, particularly, Makran region (Altamimi et al., 2012; Frohling and Szeliga, 2016). The global and regional plate assemblages in southern Pakistan and southeastern Iran, geodetic constraints and earthquake focal mechanisms suggested the ongoing oblique extension at Murray ridge with a rate of ~ 3.1 ± 0.7 to 3.7± 0.7 mm/yr at southern part, however, to its northern part the Owen Fracture Zone exhibit the dextral strike –slip motion at a rate of 2-4 mm/yr along the Murray ridge (Minshull et al., 2015). An integrated study of GPS measurements (from 20 stations located in southern Iran, southwestern Pakistan and Oman) coupled with hypocentral depths expound the Makran subduction zone accumulating strain at a rate of between 17.1 $^{+4.1}_{-3.5}$ mm/yr (Frohling and Szeliga, 2016). The Chaman– Ornach-Nal fault demonstrate the western margin of Indian plate with the Eurasian plate on terrestrial part of southern Pakistan. At this margin, the accumulating interseismic strain was computed using sensitive GPS and InSAR data and Szeliga et al., (2012) concluded that variation in creeping block velocities, for instance, across Chaman fault the convergence rate was 14.1 to 19.5 mm/yr while the avg. compression velocity near southern node of Ornach-Nal fault (nearby shore) was 15.1 mm/yr.

Apropos to recent plate kinematics and strain statistics in southern Pakistan, Smith et al., (2013) anticipated a major earthquake Mw 8.8 to Mw 9.2, probably located at the megathrust of Makran. However, low seismicity at frequent rate in Makran (10-15 per month) lulled the expected projections but the rigorous mechanical work done during orogenesis of Kirthar-Sulaiman ranges, deformation of ophiolitic belt of Balochistan and sedimentary mountainous terrains off the onshore Makran during geological times (Ul-Hadi et al., 2013; Khan and Khan, 2017) shall make the projected assumptions about earthquake strength inevitable. The study of Khan and Ali (2020) revealed that lowness of b-values in seismogenic pockets of southern Pakistan that may help in locating the epicenter of future sizeable earthquake in southern Pakistan. Furthermore, the ongoing increase in inter-seismic gap between potential event(s) at key faults in study area is also alarming which motivates to study the current seismicity datasets using appropriate methods (Rani et al., 2011; Szeliga et al., 2009) which is necessary to investigate the seismic hazard of individual fault accompanied by robust seismotectonic margins in southern Pakistan. The objectives of present study were: 1) to examine the seismicity in association with the individual faults 2) to identify the earthquake characteristics of each fault line in southern Pakistan and to model the spatial clustering (of peculiar magnitude levels).

The capabilities of geographical information system (GIS) are valuable for geospatial modelling of earthquake data by utilizing spatial statistical analysis tools. The Kernel Density Algorithm (KDA) is a nonparametric spatial interpolation method applied to analyze first-order properties of spatial data distribution i.e. earthquake events by computing the event's density i.e. magnitude per unit area of ground (Kagan and Jackson, 1994; Woo, 1996; Botev et al., 2010). KDA considers the point data of earthquake and anxious fault segment produced specific magnitude strengths while calculating the Kernel density (KD). The general expression of KD in two-dimensional space is given by:

$$\text{KD (s)} = \sum_{i=1}^{n} \frac{1}{\pi r^2} k\left(\frac{d_{is}}{r}\right)$$

where KD (s) is the density at location s, r is the search radius or bandwidth of the KDA, n is the number of sampling points, and k is the weight of a point i at distance dis to location s. The surface value is the peak measured at the location of point and reduces with increasing distance from the point, reaching zero at the search radius distance from the point. The variable k is usually modeled as a kernel factor of the ratio between d_{is} and r. The thematic surface models of Kernel Density are valuable in determination of area under seismic influence, spatial changes in seismicity strength, investigation of source zone characteristics, explore spatial patterns associated with tectonic and other processes, earthquake engineering and hazard analysis (Ramanna and Dodagoudar, 2012; Stock and Smith, 2002).

Dataset and Methods

The compilation of earthquake data and preparation of catalogs (earthquakes, fault geometries, faults kinematics), estimation of seismicity index to encode the seismological conductivity of faults and presentation of seismicity map layouts were complimentary tasks of this study.

i) Earthquake Data Preparation

The primary data of earthquakes was accessed from open source earthquake databases of US Geological Survey and Pakistan Seismic Network of Pakistan Metrological Department. The dataset of 4031 events (spreading over 7 ºN to 32º N and 55º E to 71º E) has been self-reviewed and annotated for cataloging. The magnitudes of those events were measured in different scales ranging between 3.7 <m< 8.1. The earthquake's catalog shall require homogeneity of magnitude type. All magnitudes scales have been translated into unified magnitude scale i.e. moment magnitude (Mw) which is considered most reliable magnitude scale for cataloging (Al-Ahmadi et al., 2014; Scordilis, 2005).

There were 3477 events out of 4031 were calibrated in mb and mblg scale, thus, homogenized to Mw by adopting the conversion relations [i.e. Mw= 0.89 x (mb) + 1.25; from $3.5 \leq mb \leq 6.2$] (Scordilis, 2005). There are 124 events having magnitude in Richter magnitude scale, which have been homogenized by conversion relation [Mw= 1.050 x (ML) + 0.520; for events 2.8 < ML< 6.5]. Remaining 52 events have been homogenized from the surface magnitude scale to the moment magnitude scale by adopting the relation {i.e. Mw= 0.63 x (M_S) + 2.21; $3.5 \leq MS \leq 8.0$} as suggested by Khan and Ali (2020). Only 9.3% of the dataset shows the magnitude strength in moment magnitude, thereby, the magnitude of 378 events earmark vis-à-vis. The secondary source of earthquake events was the Mw-based unified catalog which present the historic events during 325 B.C. to 1900, of southern Pakistan and frontal offshore areas. There were 428 such events before the instrumental age of earthquake recording i.e. pre-1900. Therefore, the historic events have been merged with the primary data inventory of this study to compile a 'final catalog' containing 4459 events unified to Mw.

This unified catalog has been methodically processed to filter noisy data i.e. foreshocks and aftershocks. The delustering exercise was performed using Reasenberg method which found 135 clusters populated with 975 events. The epicenters out-lying the spatial boundary of study area were 341, thus removed from the catalog. Thereby, the filtered events in the 'final catalog' were reduced to 3275 occurred during the period of 325 B.C. to 2020 February, 16. The estimated magnitude of completeness (Mc) for final catalog was Mw 5.3 (at max. curvature solution), however, the threshold magnitude of catalog was Mw 3.7. The focal depth of the catalog varies from 0 km to 121 km.

ii) Allied dataset

The land and sea surface topography of southern Pakistan has been archived from the global terrain model for ocean and land (GEBCO) (www.gebco.net/data_and_products/gridded_bathymetry_data/gebco_2019). The global gridded bathymetric dataset is presenting topography at 15 arc-second intervals (accessed on 15 Feburary 2020). The digital boundaries of transform and subduction plates were accessed in ArcMap format from the global project of Coffin et al., (1997). An inventory of geological fault lines in southern Pakistan has been developed after digitization of georeferenced structural maps of previous studies. The fault line geometries were stored as vector layer in ArcGIS format. The parameters of fault plane were quested from the Global Centroid Moment Tensor (CMT) database for major earthquakes (M>5.0) occurred in the southern Pakistan (Dziewonski et al., 1981; Ekström et al., 2012).

iii) Dataset utilization

A matrix of 3278 x 9 was prepared for estimation of Mc and b-values by maximum curvature solution, using Zmap application. These seismicity variables are vital to retrieve probabilistic future seismicity and important in defining the seismicity index. The capabilities of ArcMap tools have been explored for data analysis, clipping and mapping of desired earthquake data. The clipping tools of ArcMap were utilized to select the events within the buffer around a fault line and tectonic lineaments. The clipping tool improve the efficiency in getting data points in response of spatial queries. Since, the primary key of earthquake dataset is the spatial coordinates of epicenter of each event. The other substantial information of events was also considered for applying bi-modal query. A simplified query model (QM) was built in ArcMap to export the spatially distributed data within buffer of potential fault line or tectonic margin**.** This query operation works like "what to select" in structured query language which is a standard computer language used for accessing and managing databases and thereby generate resultant vectors data (desired point layer). The QM for each fault generated the numbers of events (Ni) lie within the buffer routing the fault geometry (polygon). Furthermore, the output of QM enabled to investigate the earthquake characteristics in cohort to the parental fault line.

Moreover, the final catalog was utilized in mapping of seismicity and modeling of earthquake data by KD algorithm, using ArcGIS. We have applied statistical-based spatial data analysis technique i.e. KDA on earthquake point data (325 B.C to February 2020). GIS-based procedure of KDA articulates Kernel density of epicenters by computing magnitude per unit area of ground. Since the epicenters of this catalog were spreading over teleseismic distances (>10 º), the 'Geodesic method' was considered instead of the 'Planar method' to maintain correct distance estimation across the latitudinal arcs. The Geodesic method considers the curvature of the spheroid, thus measure precise area-based density of epicenters. The KD models were projected at datum of WGS 1984 spheroid (semi-major axis: 6378137.0; semi-minor axis: 6356752.314245179 and inverse flattening factor: 298.257223563). The KD models for each magnitude class of earthquake events were presented as a raster surface graded in pixel values (KD value) encoded with specific color spectrum.

Results and Discussion

The outlook of regional seismicity manifests that the seismicity is well populated over the mosaic of lithospheric plates in study area (Fig.1). Despite seismotectonic margins of Indian, Eurasian and Arabian plates, the intraplate regions also share paramount contribution to the seismicity yield of the region. It is revealed that the epicenters of earthquake events lie on intraplate regions of Eurasian plate were in majority (~60% of the total events) whereas the Arabian plate and Indian plate contribute 22% and 18%, respectively. It was speculated that the interplate margins of plates with the Eurasian plate are feeding more seismic fuel as seismic stresses to promulgate in intraplate regions of assorted lithospheric mosaic. It is presumably true that these margins were undergone brittle deformation and yield subsequent seismicity. The elastic stresses received from conjugate push & pull tectonic environments, the local creeping of the blocks has integral role in clustering of intraplate earthquakes and pattern definitions in the southern Pakistan. The seismic patterns help to present an insight of active seismotectonic zones of intraplate regions in southern Pakistan.

It was aimed to delineate the seismicity profiles at high spatial resolution of various seismotectonic zones in southern Pakistan. The seismogenic fault lineaments are providing a base map grid to study the seismicity characteristics of individual fault response. The seismotectonic of the region is better understood with deep analysis of earthquake data and the seismicity patterns in association with characteristics of the faults (Szeliga et al., 2009; Smith et al., 2013) (Fig.2)

The earthquake epicenters of moderate-to-major magnitude neatly follow the trends of plate margins particularly at Carlsberg ridge to the south and Murray ridge in offshore area of study area. However, few events are dispersed with the widening of Murray ridge at its middle part. The moderate magnitude earthquake epicenters alleviate at eastern side (along the transform Ornach-Nal fault probably coupling with Murray ridge), however, the seismicity mounting at western side (probably pairing of subductions thrust with Minab transform fault).

The earthquake epicenters are asymmetrically clustered along the longitudes of Makran subduction zone, though, the clusters are in an equilibrium of the subduction thrust's seismicity, the epicenters were multitude at middle longitude (near Pak-Iran border in offshore) which add more gravity to degree of deformation at middle segment of the subduction thrust, these clusters probably marked locked Arabian slab along the wide-angle arc at Makran subduction zone. Similarly, massive deformation along collisional western margin of Indian plate, particularly in the Sulaiman lobe (northeastern part of Balochistan) the tertiary rocks rocked the study area with amassed clusters. A detailed geophysical study is suggested in offshore environment to map the interlocking pockets of Arabian slab; moreover, the interlinking configuration of subduction thrust with the boundary transform fault zones on both sides (Pakistan, near Karachi) and Minab (Iran). The interpretation of seismic surveys coupled with bathymetric profiles may shed some light to exhume the interlinking of faults entering from coastal belt to near-shore (subduction zone, Murray Ridge, Tripple Junction) camouflaged, yet.

A careful screening of seismic events concurrence to the fault lines helped us to examine the seismicity parameters associated with each fault line in study area. These parameters were included: Moment magnitude (Max, Min), focal depth (Shallow, Deep), credible mag date, seismicity pattern cluster (along the trend line). Though, a rigorous effort was made to abstract comprehensive information related to fault dynamics, slip rate, length, orientation, while subsequent earthquake characteristics from literature review of studies such as Mokhtari et al., (2019); Bilham et al., (2007); Altamimi et al., (2012); Frohling and Szeliga, (2016); Martin and Kakar, (2012); Smith et al., (2013); Szeliga et al., (2012); Ul-Hadi et al., (2013) (Table-1).

The estimation of the recurrence period for credible magnitude along the key faults was estimated by equation -I.

$$Tr = (T^{\circ} \times 10^{b(M-M*)}) / N \qquad \text{Equation-I}$$

Tr = Recurrence Time Period in years
T^{o} = Observational Time Period in years

M* = Magnitude of Completeness (Mc) i.e. Mw=5.3
N = Cumulative Number of Earthquakes of Magnitude M* and above.
M = Maximum Credible Magnitude on the fault line

Tr is estimated return period, considering 50 years on avg. for active observations in study area. The b-values were estimated, using the maximum curvature solution of data points. The statistical procedure of curvature solution considers best-fitting of a master-line at frequency-magnitude-distribution plot of the dataset and determined the Mc and subsequently b-values as factors of best-fitted slope at max. curvature (Ashadi et al., 2015). The b-value estimation are integral component for Tr estimations.

An updated dataset was summarized for each key fault line e.g. active segment length of fault, major and minor magnitude, shallowest and deepest hypocenter, estimation of recurrence period for credible magnitude Mmax in 50 years of observations, etc. This database was further used to define a seismicity index (SI) for the first time in southern Pakistan. SI ranked the key fault lines with their seismogenic potential and seismotectonic characteristics which may help in hazard mitigation. Since recurrence interval depends on the number of events, max magnitude of fault, Mc, b-value, thus Tr is considered to define the cut of limits for SI i.e. SI=I for Tr< 50 years; SI=II for 51<Tr< 100 years; SI=III for 101<Tr< 200 years, SI=IV for 201<Tr< 500 years SI=V for Tr> 501 years.

The faults Kathiwar, Bhuj, Surjan, Gaj, Kirthar, Mughal Kot, Kingri, Pardan, Harnai, Ziarat, Ghazaband, Sonmiani, Nai Rud, Kulri, Murray Ridge, Ornach Nal fault were recognized as more sensitive faults grouped as rank-I (low values of SI reflects, more susceptible to earthquake). High SI ranked the Makran subduction zone, Kalat, Mach, Dalbandin and Malik Salar fault zones inferred to undergo seismicity in longer duration. Although, the recurrence interval is necessary for seismic hazard assessment and predicting an earthquake in an area. The projecting earthquake estimations shall be précised with fault kinematics in it most immediate surroundings, fault mechanics and differential slip rates along the suspected potential fault (Papazacho et al., 2004). The faulty regions characterized with low b-values are more vulnerable to future earthquakes in Makran region (Rani et al., 2011).

The spinel interpolation method is useful for making smooth interpolation surface of the data points widely distributed. Geoprocessing tool of ArcMap employed the spinel interpolation algorithm to compute interpolates from points using a minimum curvature spline technique (Scott and Janikas, 2010). The GPS velocities of creeping faulty blocks in Makran region has been observed by Altamimi et al., (2012). The interpolation of velocity components show the relative changes across the faulty blocks e.g. transform Chaman fault, Gahzaband fault, Makran subduction zone (Fig 3 a & b). The seismic velocities are significantly varying within local coordinates help to distinguish relatively dynamic faulty blocks to the northeast of study area. Wherein, complex geological processes augment seismotectonic stress accumulation/release processes evident from the creeping velocities and high density of earthquake events in different pockets. It is suggested to establish advanced earthquake stations for monitoring and determination of continuous stresses, deformation rates, lithospheric kinematics at high resolution along the mega seismotectonic margins, i.e. oceanic-continent convergence at Makran, ocean–continent oblique transform motion at Murray ridge and continent-continent collision at western margin of Indian plate in the study area

The dearth of seismometers or accelerometers installed in Sindh and Balochistan regions preclude the mapping of stresses being accumulating in various faulty blocks. It is challenging to know the fault block is either creeping or locked by interpolation of hypocentral depths and GPS velocities. With these limitations, it may be basic but credible to investigate the source parameters of earthquakes as possible geophysical information of the faulty areas. Contrary to creeping of the blocks, the locking segments are 'more vulnerable' and alarming due to experiencing interseismic stage and accumulating stresses rather releasing minor earthquakes. These seismicity approaches considering platform velocities, geometries of faulty blocks, epicentral patterns, reckoning of potential fault strength, b-values and recurrence interval etc. are helpful in hazard assessment (Chen et al., 1998).

ii) Spatial analysis of Epicenters of magnitudes

Since the study area is seismically active, diversified in seismogenic potential, earthquake born processes, and consequential variation in magnitude strengths of the earthquakes. The magnitude of earthquakes quantifies the amount of elastic strain energy released during the earthquake. It was revealed that the changes in magnitude strength are not just the statistical data variations, but these changes are closely articulated with the seismo-geological characteristics, deformation and depth of the active fault segments, microseismic proximity to the active margins, structural stability, faut mechanics and its kinematics etc. The catalog of earthquakes is fragmented into magnitude classes (Table-2).

The KD algorithm generated continuous raster maps of earthquake density in a nexus of the faulty blocks, by computing the locations of earthquake concentration and respective magnitude values. Higher number of events with higher magnitude will give high density values and vice versa. KD maps show significant changes in spatial patterns of earthquake epicenters for respective magnitude classes (Fig 4). Henceforth, the KDF map illuminate active seismotectonic pockets with contrasting buffers of kernel density to isolate the anomalies from background values, elucidate the individual fault response in different magnitude classes which may be subsequently ascertain the seismicity potential in future. aseismic segment/spatial locking

The epicenters of main shocks (M_w 3.0 to M_w 4.0) were concentrated to the Minab fault (Iran). However, this magnitude class is often populated with the aftershocks and foreshocks in any region. The declustering exercise identified and remove the noisy data cloud of micro-seismicity (aftershocks and foreshock having Mw<4.0) masked the clusters of moderate & high magnitude events.

The KD map (Fig.4a) for earthquakes having Mw 4.0 to 5.0 have highest Kernal density at western segment of Carlsberg ridge, northwestern Minab fault, Ghazaband fault, Runn of Kucth and along the periphery of the Sulaiman lobe. The anomalous KD highlight two areas of southern Pakistan i.e. faulted blocks of Sulaimna lobe (Balochistan) and Runn-of-Kutch (Sindh). The faults of Sulaiman lobe are characterized with thrust & reverse, penetrated deep beyond the basement decolment, however, the offshoots of reverse faults disturbed the Tertiary rocks to host shallow depth moderate magnitude events. Thus, KDA computes a 'horizontal Kidney' subparallel to the curvilinear margin of Eurasian-Indian plates. The high KD in RoK zone squeezed with in local ruptured zone i.e. Bhuj faults, Banni Fault, Kutch mainland fault. However, the KD drops immediately while entering Indus Delta and southeastern Sindh. The contours of low KD values frilling in outskirts of Kirther range extending to the southern Part of Blaochistan and Sindh. Similarly, these low KD spheres outreach to the southeastern Iran from the Minab fault zone. However, the northwestern Balochistan is quite to Mw 4.0 to 5.0. Least KD values to the lower part of Awaran near coast which break the continuity of moderate KD contour extending from coast to Murray ridge. Moderate KD values distinguished the stresses along the curve of Murray ridge, probably representing a 'sho-knot' in shallow depths.

KD trends for main shocks of Mw 5.0 to 6.0 are forming connecting surfaces spreads over southern Pakistan (Fig. 4b). The dimensions of low KD surface is depicting the appearance of 'low-level stratus' clouds. There are four elliptical patches of low KD for earthquakes 5<Mw<6 magnitude along the Murray ridge segments. Three vulnerable pockets identified with high KD located to the convex of western margin of Indian plate (beginning of the Sulaiman lobe curvature) and convex of Minab fault (Iran). Least KD values (for Mw 5.0 to Mw 6.0) highlights the Carlsberg ridge, offshore Arabian sea, Indian ocean and northwestern Balochistan. The progressively decreasing KD contours in the vicinity of Quetta and Khuzdar outsourced from high KD peaks. The moderate KD values prominent in the Pasni & Gwadar region, Bhuj, Nasratabad (Iran). Interesting to notice that kernel density is that the density of higher magnitude earthquakes increases in terrestrial part of southern Pakistan (Fig 4b). This shows that southern part has low frequency of earthquakes but processes higher probability of higher magnitude of earthquakes. All these parameters clear the picture that northern part can be said as the central eye of the earthquake events. The connection or extension of faults such as Hoshab and Panjgur in Iran faults nearby splays of Nasratabad fault need to be investigated with more data. Similarly, the coupling of transform fault i.e. Ornach- Nal fault with the Murray ridge and uncertainty of the triple junction are suggested to investigate.

It is significant to notice that the Murray ridge shows least KD values for 6.0<Mw<7.0, however the junction of Murray ridge and Carlsberg ridge elucidate with higher KD values for high magnitude events (Fig. 4c). The size of higher KD spheres increase for high magnitude events at four benchmarks illuminated at Pasni-Gwadar region, Kallat, Sulaiman-lobe and Minab (Iran). High to moderate KD values show 'active segments' with high yield of events for this class. Least KD for higher magnitude events helped to detect 'locked or aseismic zones' along the seismotectonic lineaments in southern Pakistan. The expending surfaces of low to moderate KD values for this class span over Sindh, except, high KD contours for high magnitude events prominent Hyderabad, Bhambore, Bhuj regions under the influence of devastating events of Sindh during historic records.

There are 19 highest magnitude events 7.0<Mw<8.1. 50% of these events occurred in historic times (pre-1900). The KD map illuminate the most vulnerable zones for the highest magnitude class. There are three closed spheres locate to the offshore areas i.e. along the Carlsberg ridge and Makran subduction zone (Fig. 4d). These contours divulge major tsunamigenic events e.g. Makran earthquake of 325 BC, 1945 & 1483 and Carlsberg ridge earthquake of 1954. The estimates for least KD values helped us to recognize 'cut-off' value for earthquake along the Murray ridge which remain silent with least KD values for 6<Mw<8. There are four elliptical spheres of higher KD values for highest magnitude event, located to the terrestrial part of southern Pakistan (Sindh and Balochistan). The downward progression of KD levels from

peak values encompasses major cities of Balochistan and northern Sindh. The epicenters of historic events in Sindh cause expansion of peak KD values in surrounding of Indus Delta (Bhambore & Hyderabad region). These high Kernel density for higher magnitude events prominent in the areas e.g. Hyderabad, Bhambore, Bhuj etc. under the influence of devastating events of Sindh during historic records.

The spatial distribution of earthquake events along active faults and Kernel Densities shows the northeastern Balochistan more significant with higher number of earthquakes and higher probability of the high-magnitude earthquake events during instrumental age. Since the area is based on vigorous movement of faulty blocks (Ambraseys and Bilham, 2003). It may be hypothesized that the low bouger gravity at high topography of Sulaiman range has higher Kernel densities computed by KD algorithm. Although, the southern region of Balochistan and Sindh has low frequency of high magnitude earthquakes in recent times, but the potential faults engendered large magnitude earthquakes in historic records are found in low seismicity index. The results of this study would contribute to mild the curiosity of people living with earthquakes and uncertainty about seismological suspects in southern Pakistan.

The seismicity off the known faults ought to clue any invisible branch or unknown fault lines (blind fault), thus seismicity trends contributed to recognize a blind threat by overlay analysis of earthquake dataset with known fault lines of the region. We have speculated unknown fault lines in southeast of Sindh, however, integration of geophysical data is suggested to know the structural geometries within deformed sedimentary cover and underlying basements rocks. The seismic surveys conducted in exploration for structural traps of hydrocarbons may help in understanding with the structural dynamics of southeastern Sindh. Wherein, the geophysical imaging facilitates to critically look-down into the 'hot-zones' to understand the degree of structural damage, and changes of brittle deformation in different seismogenic pocket. Yet the seismogenic faults are more pronounced and sensitive for developers and policy makers. The seismicity index of potential faults in the region may help in designing tangible measures against seismicity hazard for major cities adjacent to highly indexed fault lines in vibrant southern Pakistan. These maps were significant to analyze spatial changes in earthquake magnitude and credible for the urban planners & developers to design earthquake resistant buildings in various parts of southern Pakistan.

Conclusion

The Mw-based updated catalog of earthquakes has been utilized to study the spatial patterns of earthquakes and their parameters colinear to the known faults in southern Pakistan. It is challenging to elucidate the seismicity parameters of each fault in active seismic zones but GIS-tools were found helpful in detail analysis. The seismicity index ranked the potential faults in rank-I. Kernel density maps (for Mw>4.0) allure the spatial patterns of earthquakes with higher magnitudes were notably concentrated in the central, northeastern and southern parts of study area. Kernel Density maps for moderate magnitude shows the spatial connectivity of shallow depth earthquakes along the extension of the fault zones in Iran, offshore Arabian sea and Balochistan.

List of abbreviations

GIS	Geographical Information System
KD	Kernel Density
KDA	Kernel Density Algorithm
Mc	Magnitude of Completeness
Mw	Moment Magnitude
QM	Query Model
SI	Seismicity Index

Declarations

Availability of Data & Material
The dataset used in this study are available with copyright.

Competing interests
There is no competing financial and non-financial interests.

Funding
Not applicable

Author Contributions Statement

Mr. Muhammad Jahangir Khan conceptualize and wrote the manuscript and prepared Figures & Tables.

Acknowledgements

The open source agencies US Geological Survey and Harvard CMT- Lamont-Doherty Earth Observatory (LDEO), GEBCO and Pakistan Metrological Department are acknowledged for providing the access to the desired datasets from their archives. The author is pleased to thankful to Prof. Dr. Mubarik Ali (Pakistan), Dr. Rolodfo Console (Italy), Prof. Dr. Roger Bilham (USA), Dr. Min Xu (China) and Prof. Mehrab Khan (Pakistan) for their valuable suggestions, motivation and technical guidance. The HoD of Department of Earth & Environmental Sciences, Bahria University Karachi Campus is also acknowledged for facilitating to conduct present study by utilizing the software resources of departmental lab.

References

1. Ainuddin, S., Routray, J. K., & Ainuddin, S. (2014). People's risk perception in earthquake prone Quetta city of Baluchistan. *International Journal of Disaster Risk Reduction*, *7*, 165-175.
2. Ali M., and Khan M. J., (2015). GIS Based Study on Seismicity of Makran Over 100 Years. Int. J. of Economic and Environment Geology, 6(2), 11-16.
3. Al-Ahmadi, K., Al-Amri, A., & See, L. (2014). A spatial statistical analysis of the occurrence of earthquakes along the Red Sea floor spreading: clusters of seismicity. *Arabian Journal of Geosciences*, *7*(7), 2893-2904.
4. Altamimi Z. Métivier L. Collilieux X. (2012). ITRF2008 plate motion model. J. geophys. Res.117 doi:10.1029/2011JB008930
5. Ashadi A. L., Harmoko U., Gatot Y., and Kaka S.I. (2015). Probabilistic Seismic-Hazard Analysis for Central Java Province, Indonesia. Bulletin of the Seismological Society of America, Vol. 105, No. 3, doi: 10.1785/0120140277
6. Aslam, B., and Naseer, F. (2020). A statistical analysis of the spatial existence of earthquakes in Balochistan: clusters of seismicity. *Environmental Earth Sciences*, *79*(1), 41.
7. Ambraseys, N., and Bilham, R. (2003). Earthquakes and associated deformation in northern Baluchistan 1892-2001. *Bulletin of the Seismological Society of America*, *93*(4), 1573-1605.
8. Azzaro, R., Bernardini, F., Camassi, R., & Castelli, V. (2007). The 1780 seismic sequence in NE Sicily (Italy): shifting an underestimated and mislocated earthquake to a seismically low rate zone. *Natural Hazards*, *42*(1), 149-167.
9. Bilham, R., Lodi, S., Hough, S., Bukhary, S., Khan, A. M., & Rafeeqi, S. F. A. (2007). Seismic hazard in Karachi, Pakistan: uncertain past, uncertain future. *Seismological research letters*, *78*(6), 601-613.
10. Botev, Z. I., Grotowski, J. F., & Kroese, D. P. (2010). Kernel density estimation via diffusion. *The annals of Statistics*, *38*(5), 2916-2957.
11. Byrne, D. E., Sykes, L. R., and Davis, D. M. (1992). Great thrust earthquakes and aseismic slip along the plate boundary of the Makran subduction zone. *Journal of Geophysical Research: Solid Earth*, *97* (B1), 449-478.
12. Chen, Y., Liu, J., Chen, L., Chen, Q., & Chan, L. S. (1998). Global seismic hazard assessment based on area source model and seismicity data. *Natural Hazards*, *17*(3), 251-267.
13. Coffin, M. F., Gahagan, L. M., & Lawver, L. A. (1997). *Present-day plate boundary digital data compilation*. Institute for Geophysics.
14. Dziewonski, A. M., Chou, T. A., and Woodhouse, J. H. (1981). Determination of earthquake source parameters from waveform data for studies of global and regional seismicity. *Journal of Geophysical Research: Solid Earth*, *86*(B4), 2825-2852.
15. Ekström, G., Nettles, M., and Dziewoński, A. M. (2012). The global CMT project 2004–2010: Centroid-moment tensors for 13,017 earthquakes. *Physics of the Earth and Planetary Interiors*, *200*, 1-9.
16. Frohling, E., and Szeliga, W. (2016). GPS constraints on interplate locking within the Makran subduction zone. *Geophysical Supplements to the Monthly Notices of the Royal Astronomical Society*, *205*(1), 67-76.
17. Kagan, Y. Y., and Jackson, D. D. (1994). Long-term probabilistic forecasting of earthquakes. *Journal of Geophysical Research: Solid Earth*, *99*(B7), 13685-13700.
18. Khan M. J. and Ali M. (2020). Assessing and Characterizing Seismicity of Southern Pakistan utilizing an Updated Earthquake Catalog. Under-Review in Annals of Geophysics.
19. Khan M., and Khan M. J., (2017). Geology and Petrography of Peridotites (Mantle Section) From Bela Ophiolite Balochistan, Pakistan. Bahria Univ. Research J. of Earth Sci. Vol. (2) 16-22
20. Khan M. J., Ali M., Khan M., (2020). Seismicity Evaluation of Major Strike-Slip Faults in Southern Pakistan. Under-Review in Acta Geophysica
21. Martin, S. S., and Kakar, D. M. (2012). The 19 January 2011 M w 7.2 Dalbandin earthquake, Balochistan. *Bulletin of the Seismological Society of America*, *102*(4), 1810-1819.
22. Minshull, T. A., Edwards, R. A., & Flueh, E. R. (2015). Crustal structure of the Murray Ridge, northwest Indian Ocean, from wide-angle seismic data. *Geophysical Journal International*, *202*(1), 454-463.

23. Mokhtari, M., Amjadi, A. A., Mahshadnia, L., & Rafizadeh, M. (2019). A review of the seismotectonics of the Makran Subduction Zone as a baseline for Tsunami Hazard Assessments. *Geoscience Letters*, *6*(1), 1-9
24. Pararas-Carayannis G., (2006) The potential of tsunami generation along the Makran Subduction Zone in the northern Arabian Sea: Case study: the earthquake and tsunami of November 28, 1945. Sci Tsunami Hazards 24(5): 358–384
25. Papazachos B. C., Scordilis E. M., Panagiotopoulos D. G., Papazachos C. B. and Karakaisis G. F. (2004). Global relations between seismic fault parameters and Moment magnitude of earthquakes. Bulletin of the Geological Society of Greece vol. XXXVI, 2004
26. Quittmeyer R.C., and Jacob K.H. (1979). Historical and modern seismicity of Pakistan, Afghanistan, northwestern India, and southeastern Iran. Bull. Seismol. Soc. Am. 69(3):773–823
27. Rani, V. S., Srivastava, K., Srinagesh, D., and Dimri, V. P. (2011). Spatial and temporal variations of b-value and fractal analysis for the Makran region. *Marine Geodesy*, *34*(1), 77-82.
28. Rajendran, K., Rajendran, C. P., Thakkar, M., and Tuttle, M. P. (2001). The 2001 Kutch (Bhuj) earthquake: Coseismic surface features and their significance. *Current Science*, 1397-1405.
29. Scordilis, E. M. (2005). Globally valid relations converting Ms, mb and MJMA to Mw. In Meeting on Earthquake Monitoring and Seismic Hazard Mitigation in Balkan Countries, NATO ARW, Borovetz, Bulgaria, pp. 11-17.
30. Ramanna, C. K., and Dodagoudar, G. R. (2012). Seismic hazard analysis using the adaptive Kernel density estimation technique for Chennai City. *Pure and applied geophysics*, *169*(1-2), 55-69.
31. Scott, L. M., and Janikas, M. V. (2010). Spatial statistics in ArcGIS. In *Handbook of applied spatial analysis* (pp. 27-41). Springer, Berlin, Heidelberg..
32. Smith, G. L., Mcneill, L. C., Wang, K., HE, J. Henstock, T. J. (2013). Thermal structure and megathrust seismogenic potential of the Makran subduction zone. Geophysical Research Letters, 40.1528-1533
33. Stock, C., and Smith, E. G. (2002). Adaptive kernel estimation and continuous probability representation of historical earthquake catalogs. *Bulletin of the Seismological Society of America*, *92*(3), 904-912.
34. Szeliga, W., R. Bilham, D.M. Kakar, and S. H. Lodi (2012), Interseismic strain accumulation along the western boundary of the Indian subcontinent, J. Geophys. Res., 117, B 08404, doi:10.1029/2011JB008822.
35. Szeliga, W., Bilham, R., Schelling, D., Kakar, D. M., & Lodi, S. (2009). Fold and thrust partitioning in a contracting fold belt: Insights from the 1931 Mach earthquake in Baluchistan. *Tectonics*, *28*(5).
36. Ul-Hadi, S., Khan, S. D., Owen, L. A., Khan, A. S., Hedrick, K. A., & Caffee, M. W. (2013). Slip-rates along the Chaman fault: Implication for transient strain accumulation and strain partitioning along the western Indian plate margin. *Tectonophysics*, *608*, 389-400.
37. Woo, G. (1996). Kernel estimation methods for seismic hazard area source modeling. *Bulletin of the Seismological Society of America*, *86*(2), 353-362.

List of Figures

Table-1 Meta data of fault lines (31) and their seismicity response, seismological characteristics in southern Pakistan.

Fault name	Seismicity Parameters (This study)								Fault Characteristics (Literature)			
	M Max	M Min	Z Max	Z Min	Date of M_{max}	High	Low	Events	Trend	b-value	Tr (Year)	SI
Chaman Fault	6.7	4.7	40	0	20 Dec1892	N	Mid	29	NE-SW	1.08±0.11	56.0	II
Ornach Nal F.	6.5	4.5	43	7	13 June 983	N	S	52	N-S	1.43±0.21	50.0	I
Hoshab Fault	7.7	4.6	52	5	24 Sep 2013	N	SW	45	NE-SW	1.04±0.14	348.1	IV
Pab Fault	6.1	4.5	65	26	2 Oct 1984	N	S	26	N-S	1.12±0.19	15.1	I
Makran Subd. Thrust	8.1	4.5	67	0	27 Nov1945	W	-	84	E-W	1.35±0.19 1.12±0.19	3586.7	V
Nai Rud Fault	5.7	4.5	33	10	13-Jan-1973	E	W	13	NE-SW	1.04±0.14	10.0	I
Mor Fault	5.9	4.8	54	19	4 Oct 1974	N	S	24	N-S	1.12±0.19	9.8	I
Murray Ridge	5.9	4.5	33	9	26 Dec1962	N	SE	97	N-S	1.27±0.17 1.19±0.19	2.7	I
Kulri Fault	5.6	4.9	54	7	25 Ma 1975	N	Mid	24	N-S	1.22±0.19	4.8	I
Sonmiani F.	5.6	4.5	33	10	25 Ma 1973	E	-	9	E-W	1.22±0.19	12.9	I
Ormara F.	6.8	4.6	33	0	31 Dec1764	-	W	7	E-W	1.12±0.19	341.9	IV
Makran W. F	6.8	4.9	35	0	19 Apr 1851	Mid	-	14	E-W	1.35±0.19	378.3	IV
Jhal Jhao F	6.1	4.9	50	10	28 Apr 1980	Mid	-	8	E-W	1.19±0.17	56.0	II
Dalbandin F.	7.2	5.1	109	19	18 Dec 2011	-	W	5	E-W	1.19±0.17	1823.9	V
Ghazaband F.	6.1	4.2	35	0	4 Mar 1990	N	S	34	N-S	0.88±0.09	7.4	I
Mach Fault	7.2	4.3	33	5	28 July1931	Mid	-	27	N-S	1.55±0.28	1631.6	V
Ziarat Fault	5.9	4.3	55	10	6 Aug 1983	E	SW	46	SW-NE	1.55±0.28	9.3	I
Malik Salar F.	7.0	4.2	88	0	9 Dec 2008	E	W	39	E-W	1.55±0.28	553.2	V
Harnai Fault	6.2	4.4	48	10	1 Feb2007	SW	E	61	SE-W	1.19±0.17	9.7	I
Khilafat Fault	7.1	4.5	35	0	27 Feb1997	S	E	43	E-W	1.19±0.17	161.3	III
Kalat Fault	7.7	4.5	38	2	27 Ma 1935	N	Mid	15	N-S	1.43±0.21	9013.2	V
Pardan F.	5.9	4.5	69	9	18 Oct 2013	N	Mid	23	N-S	1.42±0.21	15.5	I
Bar Khan F.	6.5	4.6	52	0	31 Dec 1984	SE	NW	46	E-W	1.52±0.22	72.5	II
Kingri F.	5.9	4.5	45	0	14 Ma 1951	S	N	37	N-S	1.52±0.22	11.0	I
Mughalkot F.	5.9	4.4	44	10	15 Sep 1952	S	Mid	27	N-S	1.13±0.17	8.8	I
Kirther F.	6.1	4.6	44	0	31 Jan 1989	Mid	S	18	N-S	1.22±0.22	26.3	I

Gaj Fault	5.4	4.7	33	10	21 Jan 1992	Mid	-	10	N-S	1.13±0.17	6.5	I
Surjan Fault	5.6	4.5	33	10	25 Nov1982	-	S	11	N-S	1.13±0.17	9.9	I
Bhuj Fault	6.1	4.5	27	0	16 June1819	E	Mid	33	E-W	0.91±0.16	8.1	I
Rann-of-Kuch (RoK)	7.6	3.7	33	0	26 Jan1961	E	Mid	38	E-W	0.91±0.16	163.0	III
Kathiwar F.	4.9	4.8	0	0	19 Jan 2003	E	Mid	8	E-W	0.91±0.16	2.7	I

Table-2: Basic statistics of the unified catalogs (Total 3275 events)

Mw Class	Events	Mean Mw	Min Mw	Max Mw	St. Dev.
3 - 4	15	3.92	3.7	4.0	0.3
4 - 5	1110	4.78	4.1	5.0	0.217
5 - 6	2029	5.37	5.1	6.0	0.216
6 - 7	105	6.43	6.1	7.0	0.29
7- 8.1	16	7.51	7.0	8.1	0.25

Figures

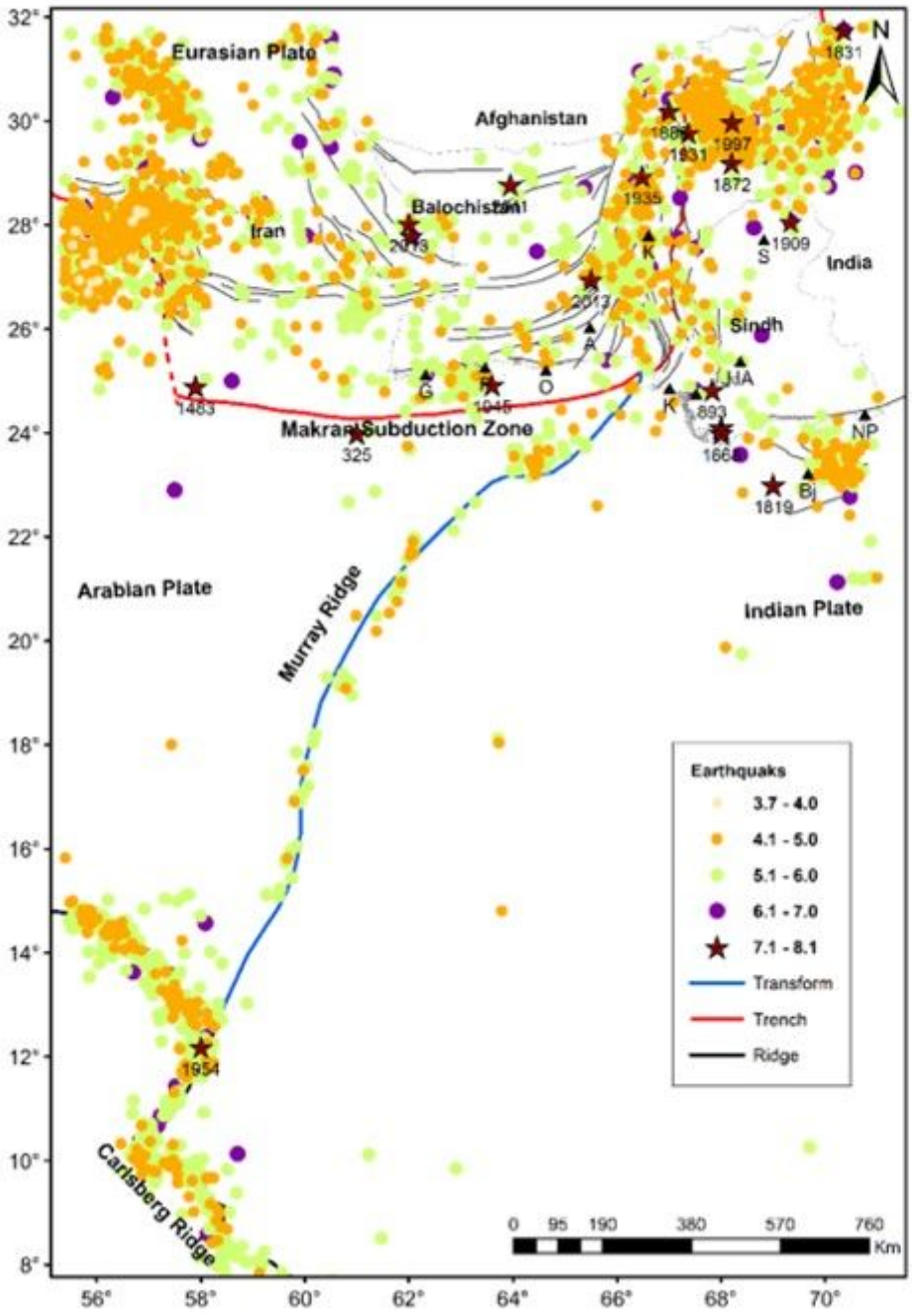

Figure 1

The seismicity distribution in study area. The regional plate margins are labeled in legends. The tectonic lineaments and fault lines are displayed in grey. The city names are: G=Gwadar P=Pasni O=Ormara K=Karachi Bj=Bhuj Np= Nagar Parkar Hy=Hyderabad S=Sukkur

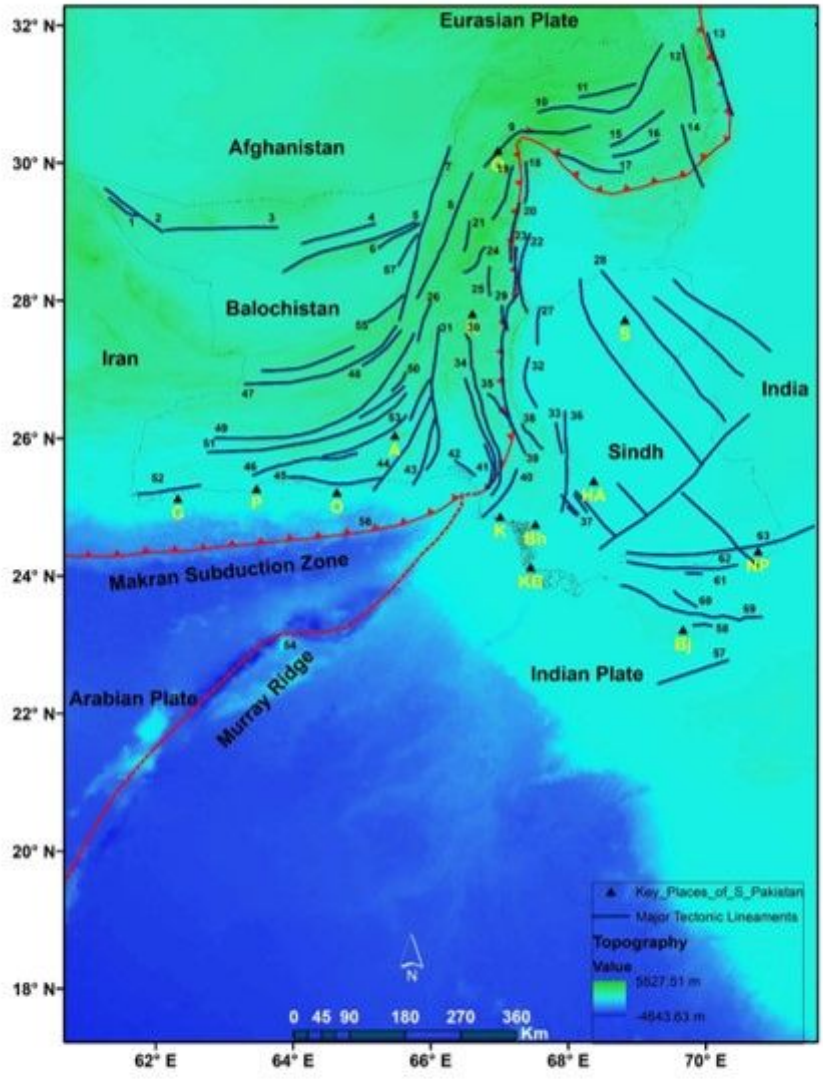

Figure 2

The development of fault lines inventory in southern Pakistan. 1) Kirtaka Fault 2) Saindak Fault 3) Mashki chah Fault 4) Dalbandin Fault 5) Ahmedwal Fault 6) Ban Fault 7) Chaman Fault 8) Ghazaband Fault 9) Malik Salar Fault 10) Zhob Fault 11) Kakarkhura San Fault 12) Mughal Kot Fault 13) Domanda Fault 14) kingri Fault 15) Murgakibzai fault 16) Kohlu Fault 17) Ziyarat-Harnai Fault 18) Mushkaf Fault 19) Johan Fault 20) Mach Fault 21) Kalat Fault 22) Gandawa Fault 23) Kotra Fault 24) Pandran Fault 25) Lehdo Fault 26) Gwani River fault 27) Karko Fault 28) Sindh plain Faults 29) Zardak Fault 30) Pab Fault 31) Ornach nal Nal Fault 32) Gaj Fault 33) Lakhni Fault 34) Mor Fault 35) Khudi Fault 36) Surjan Fault 37) Jhimpir fault 38) Bhit Jant fault 39) Kirthar Fault 40) Hub Fault 41) Windar 42) Son Miani fault 43) Aghor Fault 44) Ras Malan 45) Ormara Fault 46) Nai Rud Fault 47) Panjgur Fault 48) Raghai Rud Fault 49) Hoshab Fault 50) Awaran Fault 51) Bazdar Fault 52) Jabl-e-Mehdi fault 53) Jhal Jhao Fault 54)

Murray Ridge Fault 55) Saihan Fault 56) Makran Subduction Zone 57) Khatiawar fault 58) Bhuj Fault 59) Kutch Mainland Fault 60) Banni Fault 61) Island Fault 62) Nagar Parkar Fault 63) Allah Band Fault

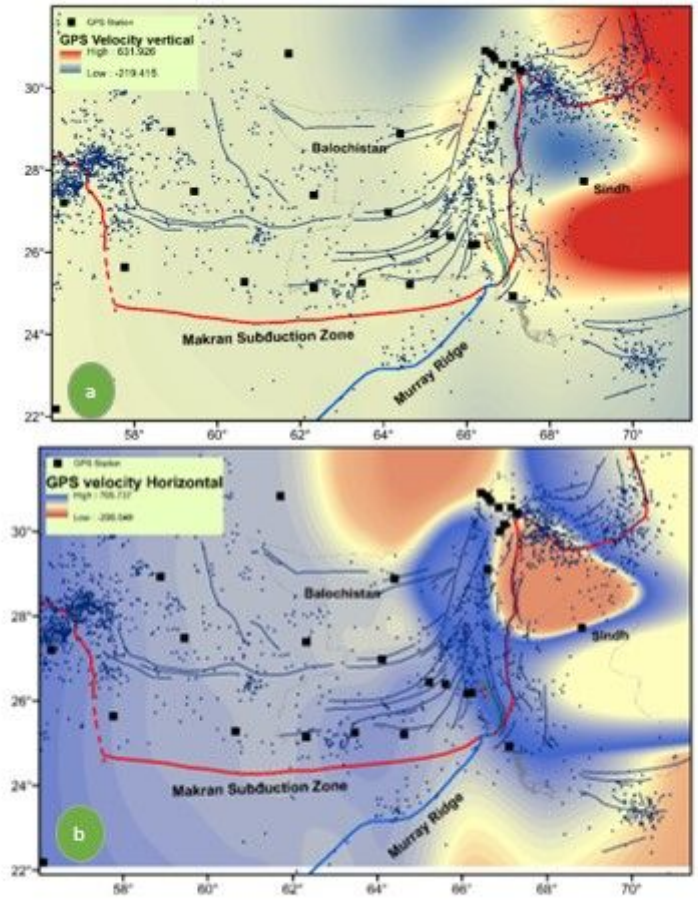

Figure 3

Interpolation maps of GPS velocities relative to the stable Eurasian plate as defined by Altamimi et al., (2012). a) vertical velocity in the study area b) horizontal velocity in the study area. The black square represents the location of GPS station.

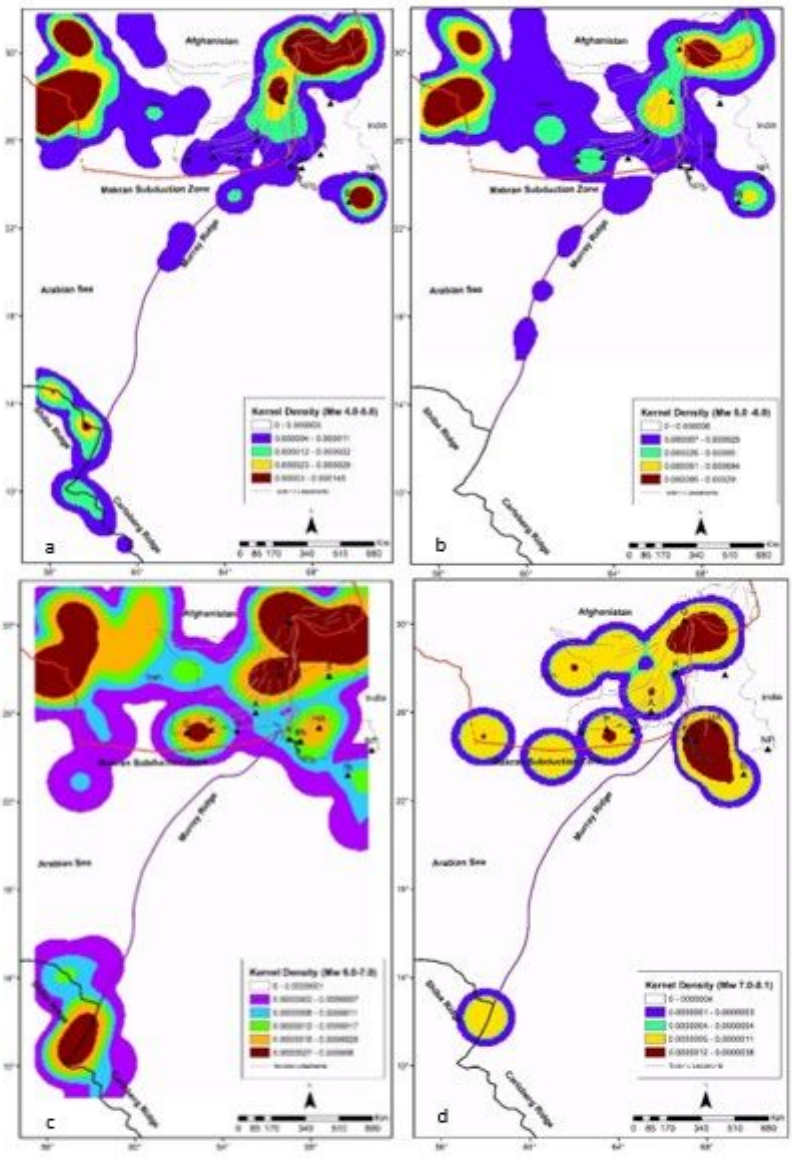

Figure 4

Kernel Density map elucidate the various pockets of faulted zones exhibiting specific strength of earthquakes. a) Mw 4-5 b) Mw 5-6 c) Mw 6-7 d) Mw 7-8.1. The calculated values of KD are classified at Natural Breaks in the range of each class, shown in color legends. If no points or line sections fall within the neighborhood of a particular cell, that cell is assigned No Data.

Supplementary Files

This is a list of supplementary files associated with this preprint. Click to download.

- Abstract.jpg